Oxygen vacancy formation energy in Pd-doped ceria: A DFT+U study

Zongxian Yang,[a),b)] Gaixia Luo, and Zhansheng Lu
College of Physics and Information Engineering, Henan Normal University, Xinxiang, Henan 453007, People's Republic of China

Kersti Hermansson[a),c)]
Materials Chemistry, The Ångström Laboratory, Uppsala University, Box 538, SE-75121, Uppsala, Sweden

(Received 9 April 2007; accepted 1 June 2007; published online 16 August 2007)

Using the DFT+U method, i.e., first principles density functional theory calculations with the inclusion of on-site Coulomb interaction, the effects of Pd doping on the O vacancy formation energy (E_{vac}) in CeO_2 has been studied. We find that E_{vac} is lowered from 3.0 eV in undoped ceria to 0.6 eV in the Pd-doped compound. Much of this decrease can be attributed to emerging Pd-induced gap states above the valence band and below the empty Ce 4*f* states. These localized defect states involve the Pd ion and its nearest neighbors, which are also the main acceptors of the extra electrons left on reduction. The effect of the Pd dopant on the geometric structure is very modest for CeO_2 but considerable for CeO_{2-x}. © *2007 American Institute of Physics*. [DOI: 10.1063/1.2752504]

I. INTRODUCTION

Increased concerns regarding environmental protection increase the demand for improvements in the automobile exhaust cleaning in many parts of the world. Three-way catalysts (TWCs) are used in automotive exhaust systems since the late 1970s and simultaneously remove NO_x, CO, and hydrocarbons from the exhaust. TWCs consist of noble metals (NM: Rh, Pd, Pt) on a metal oxide support. Here ceria (CeO_2) is a key component thanks to its favorable redox properties,[1,2] and an increase in the number and mobility of oxygen vacancies in ceria has been found to enhance its oxygen storage capacity as well as its catalytic activity.[3] Ceria reduction has experimentally been found to be promoted either by noble metal deposition or by chemical modification with one or more dopants.[4–6]

Only a small number of calculations for reduced ceria performed with the DFT+U method have been reported in the literature, for example Refs. 7–9. With the same method, we have earlier studied Zr-doped bulk ceria, where we found that the O vacancy formation energy was reduced by approximately 30% due to the Zr dopant, and the excess electrons were captured by two Ce ions neighboring the oxygen vacancy.[8] In the present paper, we will investigate the electronic structure of *Pd-doped ceria* ($Ce_{0.97}Pd_{0.03}O_2$) and its *reduced* counterpart, with special focus on how the doping affects the reduction properties of ceria. Both Pd and ceria are key components of TWCs and the combination of Pd with CeO_2 has been found to make the TWC highly active in the oxidation of CO and C_3H_6 at low temperature.[10] A good deal of information is available in the literature for Pd/CeO_2.[10–17] Some experimental results[11,18,19] give indications of NM diffusion into the ceria support. Imamura *et al.*[18] showed that Pt interacts very strongly with ceria, indicating the possibility of the formation of Pt–O–Ce bonds and the penetration of Pt into the bulk ceria. Bernal *et al.*[11] suggested that metal decoration phenomena occur on the three NM/CeO_2 catalysts. Sun *et al.*[19] reported the observation that Pd particles sank into the ceria-zirconia support after reduction. We are not aware of any electronic structure calculations of NM-doped ceria in the literature and the effects of NM diffusion as dopants into the ceria support are not clear yet. In this paper, we present a first principles study on the effects of a Pd dopant in bulk ceria.

The computational details are presented in Sec. II. The calculated results are presented in Sec. III, which discusses the effects of Pd doping on (i) the oxygen vacancy formation energy (Sec. III A), (ii) the atomic structure of undoped ceria (Sec. III B), (iii) the electronic properties of unreduced and reduced ceria (Sec. III C), and (iv) the atomic structure of reduced ceria. A brief summary is given in Sec. IV.

II. METHODOLOGY

A. Description of the model systems

Bulk crystalline CeO_2 has the fluorite structure, with each Ce^{4+} cation coordinated by eight equivalent O^{2-} ions in a cube, and each O^{2-} anion tetrahedrally coordinated by four Ce^{4+} ions. Our calculations for *stoichiometric ceria* give an equilibrium lattice parameter of 5.480 Å; the experimental value is 5.411 Å.[20]

In this study, a standard-size supercell (96 atoms) was used, built from the conventional 12-atom cubic unit cell of CeO_2 with a $2\times2\times2$ replication. *Unreduced* Pd-doped ceria was then modeled by introducing one Pd doping atom to substitute one Ce atom in the supercell, corresponding to a dopant concentration of 3%. The doped system was assumed to keep the cubic structure and the cell parameter and atomic positions were optimized, giving virtually no change in cell

[a)]Authors to whom correspondence should be addressed.
[b)]Electronic mail: yzx@henannu.edu.cn
[c)]Electronic mail: kersti.hermansson@mkem.uu.se

parameter. The resulting value was 10.955 Å for a $2\times2\times2$ supercell. The smallest vacancy-vacancy distance in our Pd-doped ceria model is thus 10.955 Å.

To create the reduced ceria and reduced Pd-doped ceria systems, one oxygen vacancy was introduced in the pure ceria supercell, and in the doped supercell, next to the Pd atom. As mentioned, the stoichiometric systems were optimized with respect to both the cell parameter and atomic positions, but the cell parameter was found to be almost constant. For the reduced systems, the cell parameter was fixed at the corresponding unreduced value.

B. Calculations

All calculations presented herein were performed with the VASP program.[21] They were all spin-polarized calculations. The valence electronic states were expanded in a basis of plane waves. The strongly oscillating wave functions of the core electrons were represented using the projector augmented wave approach. The Perdew-Burke-Ernzerhof functional[22] was used for the exchange correlation. In this paper, the DFT+U method was chosen because it has been shown that generalized gradient approximation–density functional theory (GGA-DFT) fails to give a correct electronic structure for reduced ceria due to the use of approximate exchange-correlation functionals,[8,17,23] while the DFT+U method[24,25] has been shown to remedy the situation for reduced ceria.[7,8,23,26] With the DFT+U method,[24,25] a Hubbard parameter U is introduced for the Ce $4f$ electrons to describe the on-site Coulomb interaction; this helps to remove the self-interaction error and improves the description of correlation effects. We have chosen a value of 5 eV for the Hubbard parameter U for all calculations presented herein as suggested by Nolan *et al.*, who stated that for $U\geqslant5$ eV, the electronic structure is essentially converged with respect to localization.[7,23] Incidentally, in test calculations on the CeO_2 bulk we found that the lattice parameter (5.48 Å) and the bulk modulus (188 GPa) are exactly the same for $U=5$ and 6 eV. The calculated oxygen vacancy formation energy (2.99 eV, as will be discussed in Sec. III A) for the undoped ceria system with $U=5$ eV, is also very close to the value (3.03 eV) with $U=6$ eV as reported in Ref. 8.

The cerium $5s$, $5p$, $5d$, $4f$, $6s$ electrons, the oxygen $2s$, $2p$ electrons, and the palladium $5s$, $4d$ electrons were treated as valence electrons. The Kohn-Sham orbitals were expanded in plane waves with a kinetic energy cutoff of 30 Ry. The Brillouin-zone integrations were performed using Monkhorst-Pack (MP) grids and a Gaussian smearing of the width of the smearing function (SIGMA)=0.2 eV. The final results were extrapolated to that of SIGMA=0 eV. A MP grid of $(2\times2\times2)$ was used for the 96-atom cells based on convergence tests for the stoichiometric, undoped bulk supercell. The structure optimizations were pursued until the force on each atom was less than 0.02 eV/Å and all components of the stress tensor on the unit cell smaller than 0.1 GPa.

III. RESULTS AND DISCUSSION

A. The effect of Pd doping on the O-vacancy formation energy

The O-vacancy formation energy (E_{vac}) has been calculated by

$$E_{vac} = E(\text{cell}_{vac}) + 1/2E(O_2) - E(\text{cell}), \quad (1)$$

where $E(\text{cell}_{vac})$ and $E(\text{cell})$ are the total energies of the optimized supercells with and without an O vacancy, and $E(O_2)$ is the total energy for the ground state of an optimized oxygen molecule in the gas phase (calculated with the same supercell size and method as the solid). A positive value for E_{vac} means that energy is needed to create the vacancy.

The calculated E_{vac} value for the *undoped ceria* system is 2.99 eV per vacancy, in good agreement with Ref. 8, and for the *Pd-doped* system 0.59 eV per vacancy. The Pd doping thus lowers the reduction energy by as much as 2.4 eV. What is the origin of this large change? In the following three sections, the Pd-induced modifications on the atomic and electronic structure of unreduced ceria and the Pd-induced structural modifications to the reduced ceria will be presented and their possible bearing on the vacancy formation energy will also be discussed.

B. The effect of Pd doping on the CeO_2 structure

The listed radii of the eight-coordinated Ce^{4+} and Pd^{2+} ions are not very different. The Ce^{4+} ionic radius is 0.97 Å (using Shannon's "IR" values, i.e., with the oxide ion's radius as the reference point[27]) and that of eight-coordinated Pd^{2+} can be estimated to lie around 1.0 Å from the listed values of 0.64 Å for four coordination[27] and 0.86 Å for six coordination.[27] Indeed, as mentioned in Sec. II A, our calculated undoped CeO_2 bulk supercell with an optimized lattice constant of 10.960 Å (two times 5.480 Å) shows only a very small decrease in the lattice constant (to 10.955 Å) upon doping with one Pd atom. Likewise, the atomic displacements around the dopant are quite small.

For the unreduced system, the displacements of the ions around the doping ion are indicated in Fig. 1. The Pd dopant causes only a slight perturbation of the structure. The metal-induced displacement of the oxygen anions in the Pd-doped system is symmetric and only about 0.06 Å (towards the Pd ion), and the displacement for the cerium cations is also symmetric and about 0.02 Å (also towards the Pd ion).

We conclude that the small structural changes induced by the Pd dopant in the unreduced structure are probably of minor importance for the Pd-induced lowering of the vacancy formation energy in ceria.

C. The effect of Pd doping on the electronic structure of ceria

We have analyzed the electronic structure of doped and undoped ceria, with and without an O vacancy. In particular, the total density of states (TDOS) (Fig. 2), the partial density of states (PDOS) (not shown), and spin density distribution (Fig. 3) will be discussed.

Figure 2(a) displays the TDOS for the *unreduced ceria*.

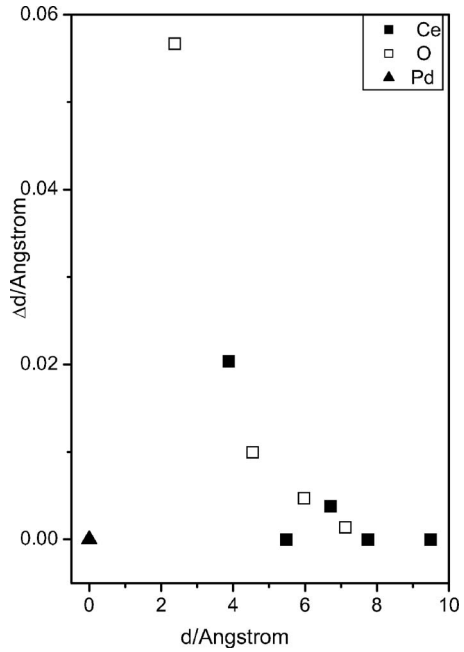

FIG. 1. Dopant-induced displacements of ions in the *Pd-doped ceria* as compared to their positions in the nondoped ceria. The horizontal axis denotes the distance of an ion from the Pd dopant. Triangle, solid, and empty squares represent the Pd, Ce, and O ions, respectively.

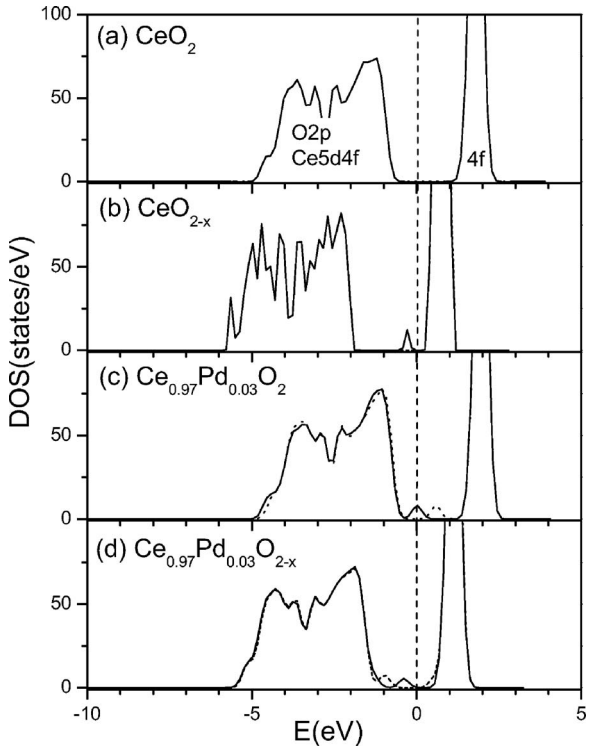

FIG. 2. Total density of states (TDOS) for (a) *unreduced ceria* (CeO_2), (b) *reduced ceria* (CeO_{2-x}), (c) *Pd-doped unreduced ceria* ($Ce_{0.97}Pd_{0.03}O_2$), and (d) *Pd-doped reduced ceria* ($Ce_{0.97}Pd_{0.03}O_{2-x}$). For the unreduced ceria systems, only the non-spin-polarized total DOS is shown, since no spin polarization is found. For the reduced systems and Pd-doped ceria systems, both the DOSs for the majority spin (solid lines) and minority spin (dotted lines) are shown. The vertical dashed line at $E=0$ eV represents the Fermi energy.

Undoped CeO_2 is an insulator. The valence band has mostly O $2p$ character with some contribution from Ce $4f5d$. The sharp peak above the valence band is from the Ce$4f$ states and the states above the empty Ce $4f$ states are due to Ce $5d$ and $6s$.

Figure 2(b) shows the TDOS for the *reduced ceria*. The insulator feature of the reduced ceria is correctly reproduced. Here a new peak appears in the O$2p$-Ce$4f$ gap, with the Fermi level located in the gap between this new peak and the empty Ce $4f$. As discussed in Refs. 8, 9, and 23, the electrons that occupy the new gap states are exactly localized on two Ce cations neighboring the oxygen vacancy, and make the two Ce^{4+} cations reduced to Ce^{3+}. Very recently, Silva *et al.*[28] applied hybrid functionals to the rare-earth oxides (ceria) and correctly predicted Ce_2O_3 to be an insulator as opposed to the ferromagnetic metal predicted by the local spin density approximation and GGA methods. This shows another possibility of using hybrid functionals (other than the DFT+U method used here) to reduce the improper self-interaction.

The TDOS for the *Pd-doped unreduced ceria* [Fig. 2(c)] is obviously affected by the doping. A feature corresponding to metal-induced gap states (MIGS) appears between the O $2p$ valence band and the empty Ce $4f$ states and the Fermi level is located in this gap state. The analysis from the PDOS shows that the MIGS are mainly composed of Pd $4d$ and O $2p$ contributions. By further analyzing the spin density of

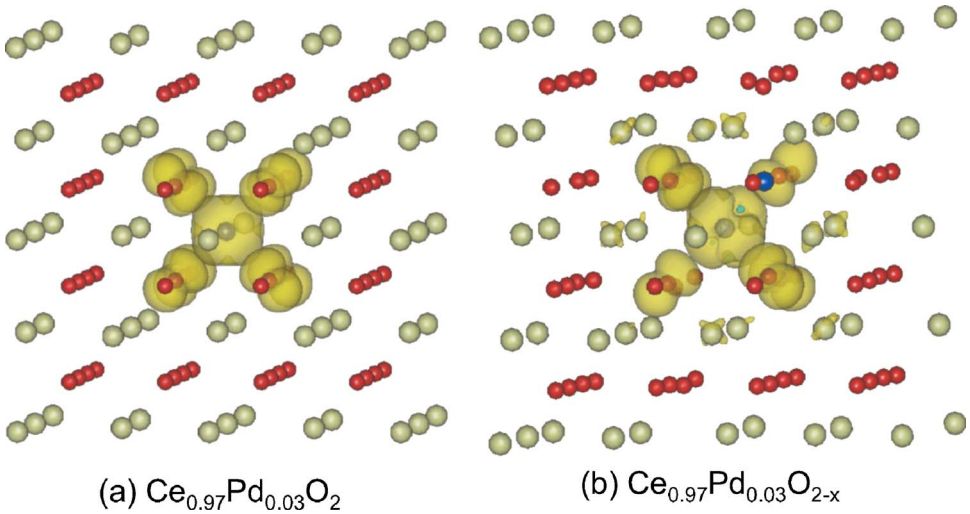

FIG. 3. (Color online) The spin density distributions for (a) the *Pd-doped unreduced ceria* ($Ce_{0.97}Pd_{0.03}O_2$) system, and (b) the *Pd-doped reduced ceria* ($Ce_{0.97}Pd_{0.03}O_{2-x}$) system. The isosurface value used is 0.01 $e/Å^3$. Here and in the following figures, yellow, purple, red, and gray spheres represent the Ce^{4+}, Ce^{3+}, O, and Pd ions, respectively. The blue spheres represent the position of a vacancy.

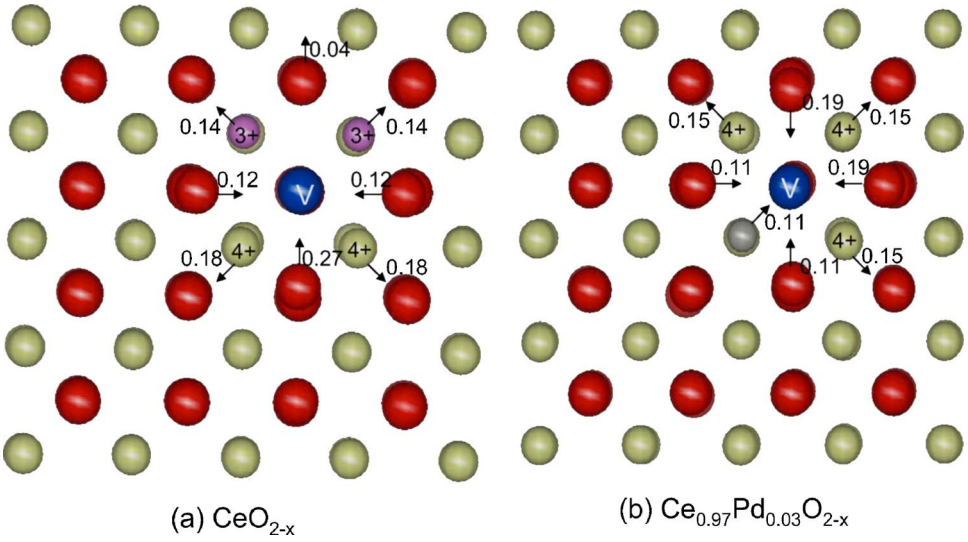

FIG. 4. (Color online) The relaxation caused by the O vacancy. The spheres show the atomic positions in the reduced systems. (a) Plane projection view showing the ionic movement for the *reduced ceria* (CeO_{2-x}) and (b) for the *Pd-doped reduced ceria* ($Ce_{0.97}Pd_{0.03}O_{2-x}$) as compared to the corresponding unreduced counterparts.

Pd-doped ceria in Fig. 3(a), we are able to identify where the net spin resides. It is mainly localized on the Pd dopant and its nearest neighbour oxygen ions. The MIGS consists of a Pd–O bonding state [solid line in Fig. 2(c)] and a Pd–O antibonding state [dotted line in Fig. 2(c)]. These partially occupied MIGS [Fig. 2(c)] offer states suitable for accommodating extra electrons.

As will be discussed in Sec. III D, the Pd ion in Pd-doped reduced ceria moves towards the O vacancy, giving the Pd dopant six nearest neighbor oxygen anions only. We find that the Pd dopant and these six oxygen neighbors take up a large part of the electrons left by the removed oxygen upon reduction. Consequently, the half occupied gap states become filled, as is seen by comparing the TDOS for the *O-deficient Pd-doped ceria* in Fig. 2(d) with the TDOS for the unreduced case in Fig. 2(c). The MIGS feature moves directly below the Fermi level; this phenomenon is obviously induced by the presence of the O vacancy. This is mainly because the gap Pd 4*d*-O 2*p* states get electrons from the O vacancy and lower their energies; this confirms the conjecture that the Pd dopant offers states suitable for accommodating extra electrons.

Using the Bader Atoms in Molecules (AIM) analysis[29] for the partial charge density corresponding to the MIGS for reduced Pd-doped ceria, we find that there are totally two electrons residing in the MIGS peak among which 0.87 electrons reside on the Pd dopant and 0.84 electrons on 6 of its nearest neighbour (NN) oxygens, and the remaining 0.3 electrons on 12 ceriums around the oxygen vacancy. By further plotting the spin density of the Pd-doped ceria in Fig. 3(b), we find that the spin density is mainly localized on the Pd dopant and its nearest neighbor oxygen anions, with a small portion localized on the nearest neighbor Ce of the Pd dopant. This is in agreement with the analysis for the partial charge density. Previous studies for either the partly covalent oxides (e.g., $SrTiO_3$) (Refs. 30 and 31) or the ionic oxides (e.g., MgO) (Ref. 32) showed that the O vacancy acts as an effective donor and a visible fraction of the electron density localizes inside the O vacancy. But this is not the case for the O vacancy in CeO_2 where the formation results in the reduction of two Ce^{4+} (to Ce^{3+}) neighboring the vacancy. We did not find any visible fraction of electrons localized inside O vacancy.

Comparing with Zr-doped ceria,[8] we observe that the Pd dopant utilizes a different mechanism to lower the reduction energy. For Pd, the location of the MIGS appears to be more important than the lattice distortions caused by Pd in stoichiometric ceria. For Zr, on the other hand, there are no new MIGS, and the electronic modification is unimportant. Therefore, the effect on E_{vac} is smaller, which is largely due to the structural distortions and subtle differences between Ce–O and Zr–O bonding.

D. The effect of Pd doping on the structure of partially reduced CeO_2

The optimized structure for reduced ceria is shown in Fig. 4(a) and the optimized structure of Pd-doped reduced ceria, with the oxygen vacancy next to the dopant, is shown in Fig. 4(b). The ionic displacements (from the positions in the respective unreduced structure) around the oxygen vacancy are also shown in Fig. 4. The displacement patterns can easily be explained in a qualitative way from the electron structure results in Sec. III C. In the case of reduced ceria, the nearest neighbors of the vacancy are two Ce^{4+} ions and two Ce^{3+} ions. In the case of our Pd-doped reduced ceria system, the nearest neighbors of the vacancy are three Ce^{4+} ions and one Pd^{1+} ion.

The nonsymmetric relaxation structure shown in Fig. 4(a) is essentially the same as our published results in Ref. 8. Thus all cerium ions neighboring the "positive" vacancy move *outwards* by 0.14–0.18 Å, and some of the vacancy's next-nearest-neighbor oxygen atoms move *inwards* (namely, those with at least one Ce^{4+} neighbor move by 0.12 and 0.27 Å) while others move outwards (namely, those with two Ce^{3+} neighbours, which move outwards by 0.04 Å).

The relaxation pattern in Fig. 4(b) is partly different. Again, the cerium ions move outwards from the vacancy by about 0.15 Å, but the Pd ion moves inwards by almost the same amount, 0.11 Å. The oxygen ions which are not neighboring the Pd dopant move inwards by 0.19 Å, while three

of the closest oxygen ion neighbors of the Pd dopant move inwards by about 0.11 Å. Probably, it is partly the electrostatic interactions that give rise to the geometric structural changes around the vacancy and the impurity, i.e., the anions moving towards the vacancy, and the cations moving away from it (with the exception of the Pd cation). The Pd impurity ion has a lower nominal valence (+2, or rather +1, since it takes up a considerable fraction of the electrons left by the released oxygen atom) than that of Ce^{4+}; this is likely to be related to the exceptional move of Pd.

The geometric relaxations shown in Fig. 4 are accompanied by large energy gains. We performed two additional single-point calculations, namely, for unrelaxed CeO_{2-x} and unrelaxed $Ce_{0.97}Pd_{0.03}O_{2-x}$; i.e., we just removed an O atom rigidly from the optimized CeO_2 and $Ce_{0.97}Pd_{0.03}O_2$ systems. The relaxation energy is 1.39 eV in the former case and 1.68 eV in the latter, i.e., 0.29 eV more in the doped case. These energy gains are already "included" in the final E_{vac} values of 2.99 and 0.59 eV for undoped and Pd-doped ceria. Considering that the total dopant-induced lowering of E_{vac} is 2.4 eV, the value of 0.29 eV is a comparatively small part. The remainder (2.11 eV) must be attributed to the changes in electronic structure induced by Pd dopant, in particular the Pd-induced gap states which lie below the empty Ce 4*f* states.

IV. CONCLUSIONS

The effects of Pd doping on the geometric and electronic structure and reduction properties of ceria have been studied using first principles density functional theory (DFT) approaches with the inclusion of on-site Coulomb interaction (DFT+U). The Pd dopant is found to have significant effects on the reduction properties of ceria. It induces a gap state peak (mostly Pd 4*d* and some O 2*p* contributions from the nearest neighbors of the dopant), which resides at the Fermi energy and is suitable for accommodating extra electrons when the O vacancy is formed, thereby lowering the O vacancy formation energy.

ACKNOWLEDGMENTS

This work was supported by the National Natural Science Foundation of China (Grant No. 10674042), the Henan Innovation Project For University Prominent Research Talents (HAIPURT: 2007KYCX004) of China, and the Swedish Research Council (VR).

[1] J. G. Nunan, H. J. Robota, M. J. Cohn, and S. A. Bradley, J. Catal. **133**, 309 (1992).
[2] K. C. Taylor, *Automobile Catalytic Converters* (Springer-Verlag, Berlin, 1984).
[3] M. Daturi, N. Bion, J. Saussey, J. C. Lavalley, C. Hedouin, T. Seguelong, and G. Blanchard, Phys. Chem. Chem. Phys. **3**, 252 (2001).
[4] P. Vidmar, P. Fornasiero, J. Kaspar, G. Gubitosa, and M. Graziani, J. Catal. **171**, 160 (1997).
[5] B. K. Cho, J. Catal. **131**, 74 (1991).
[6] P. Fornasiero, R. Di Monte, G. R. Rao, J. Kaspar, S. Meriani, A. Trovarelli, and M. Graziani, J. Catal. **151**, 168 (1995).
[7] M. Nolan, S. C. Parker, and G. W. Watson, Surf. Sci. **595**, 223 (2005).
[8] Z. Yang, T. K. Woo, and K. Hermansson, J. Chem. Phys. **124**, 224704 (2006).
[9] S. Fabris, S. de Gironcoli, S. Baroni, G. Vicario, and G. Balducci, Phys. Rev. B **71**, 041102/1 (2005).
[10] H. C. Yao and Y. F. Yu Yao, J. Catal. **86**, 254 (1984).
[11] S. Bernal, J. J. Calvino, M. A. Cauqui, J. M. Gatica, C. Larese, J. A. Perez Omil, and J. M. Pintado, Catal. Today **50**, 175 (1999).
[12] T. Bunluesin, R. J. Gorte, and G. W. Graham, Appl. Catal., B **15**, 107 (1998).
[13] C. D. Leitenburg, A. Trovarelli, and J. Kaspar, J. Catal. **166**, 98 (1997).
[14] T. Bunluesin, R. J. Gorte, and G. W. Graham, Appl. Catal., B **14**, 105 (1997).
[15] H. W. Jen, G. W. Graham, W. Chun, R. W. McCabe, J. P. Cuif, S. E. Deutsch, and O. Touret, Catal. Today **50**, 309 (1999).
[16] W.-J. Shen and Y. Matsumura, J. Mol. Catal. A: Chem. **153**, 165 (2000).
[17] S. Fabris, S. de Gironcoli, and S. Baroni, Phys. Rev. B **72**, 237102 (2005).
[18] S. Imamura, T. Higashihara, Y. Saito, H. Aritani, H. Kanai, Y. Matsumura, and N. Tsuda, Catal. Today **50**, 369 (1999).
[19] H. P. Sun, X. P. Pan, G. W. Graham, H.-W. Jen, R. W. McCabe, S. Thevuthasan, and C. H. F. Peden, Appl. Phys. Lett. **87**, 201915 (2005).
[20] L. Eyring, *Handbook on the Physics and Chemistry of Rare Earths* (North-Holland, Amsterdam, 1979).
[21] G. Kresse and J. Furthmuller, Comput. Mater. Sci. **6**, 15 (1996).
[22] J. P. Perdew, K. Burke, and M. Ernzerhof, Phys. Rev. Lett. **77**, 3865 (1996).
[23] M. Nolan, S. Grigoleit, D. C. Sayle, S. C. Parker, and G. W. Watson, Surf. Sci. **576**, 217 (2005).
[24] V. I. Anisimov, J. Zaanen, and O. K. Andersen, Phys. Rev. B **44**, 943 (1991).
[25] S. L. Dudarev, G. A. Botton, S. Y. Savrasov, C. J. Humphreys, and A. P. Sutton, Phys. Rev. B **57**, 1505 (1998).
[26] S. Fabris, G. Vicario, G. Balducci, S. de Gironcoli, and S. Baroni, J. Phys. Chem. B **109**, 22860 (2005).
[27] R. D. Shannon, Acta Crystallogr., Sect. A: Cryst. Phys., Diffr., Theor. Gen. Crystallogr. **A32**, 751 (1976).
[28] J. L. F. D. Silva, M. V. Ganduglia-Pirovano, J. Sauer, V. Bayer, and G. Kresse, Phys. Rev. B **75**, 045121 (2007).
[29] G. Henkelman, A. Arnaldsson, and H. Jónsson, Comput. Mater. Sci. **36**, 254 (2006).
[30] R. Astala and P. D. Bristowe, Comput. Mater. Sci. **22**, 81 (2001).
[31] D. Ricci, G. Bano, G. Pacchioni, and F. Illas, Phys. Rev. B **68**, 224105 (2003).
[32] Z. Yang, G. Liu, and R. Wu, Phys. Rev. B **65**, 235432 (2002).